

Lévy flights in confining environments: Random paths and their statistics

Mariusz Żaba, Piotr Garbaczewski and Vladimir Stephanovich

Institute of Physics, University of Opole, 45-052 Opole, Poland

(Dated: October 17, 2018)

We analyze a specific class of random systems that are driven by a symmetric Lévy stable noise. In view of the Lévy noise sensitivity to the confining "potential landscape" where jumps take place (in other words, to environmental inhomogeneities), the pertinent random motion asymptotically sets down at the Boltzmann-type equilibrium, represented by a probability density function (pdf) $\rho_*(x) \sim \exp[-\Phi(x)]$. Since there is no Langevin representation of the dynamics in question, our main goal here is to establish the appropriate path-wise description of the underlying jump-type process and next infer the $\rho(x, t)$ dynamics directly from the random paths statistics. A priori given data are jump transition rates entering the master equation for $\rho(x, t)$ and its target pdf $\rho_*(x)$. We use numerical methods and construct a suitable modification of the Gillespie algorithm, originally invented in the chemical kinetics context. The generated sample trajectories show up a qualitative typicality, e.g. they display structural features of jumping paths (predominance of small vs large jumps) specific to particular stability indices $\mu \in (0, 2)$.

PACS numbers: 05.40.Jc, 02.50.Ey, 05.20.-y, 05.10.Gg

I. INTRODUCTION

Many random processes in real physical systems admit a simplified description based on stochastic differential equations. In such case there is a routine passage procedure from microscopic random variables to macroscopic (statistical ensemble) data. The latter are encoded in the time evolution of an associated probability density function (pdf) which is a solution of a deterministic transport equation. A paradigm example is the so-called Langevin modeling of diffusion-type and jump-type processes. The presumed microscopic model of the dynamics in external force fields is provided by the Langevin (stochastic) equation whose direct consequence is the Fokker-Planck equation, [1] and [2]. We note that in case of jump-type processes the familiar Laplacian (Wiener noise generator) needs to be replaced by a suitable pseudo-differential operator (fractional Laplacian, in case of a symmetric Lévy-stable noise).

We pay a particular attention to jump-type processes which are omnipresent in Nature (see [3] and references therein). Their characterization is primarily provided by jump transition rates between different states of the system under consideration. However our major focus is on a specific class of random systems which are plainly incompatible with a straightforward Langevin modeling of jump-type processes and, as such, are seldom addressed in the literature.

To this end we depart from the concept, coined in an isolated publication [4], of Lévy flights-driven models of disorder that, while at equilibrium, do obey detailed balance. The corresponding research line has been effectively initiated in Refs. [5]-[7]. It has next been expanded in various directions, with a special emphasis on so-called Lévy-Schrödinger semigroup reformulation of the original probability density function (pdf) dynamics, [6, 15, 16] and [8]-[13], c.f. also [14-16]. We note in passing that the familiar Fokker-Planck equation can be equally well

formulated in terms of the Schrödinger semigroup and this property is universally valid in the standard theory of Brownian motion, [1, 14]. Its generalization to Lévy flights is neither immediate nor obvious. It is often considered in the prohibitive vein following [17, 20].

In fact, in relation to Lévy flights, a novel fractional generalization of the Fokker-Planck equation has been introduced in Refs. [5]-[7] to handle systems that are randomized by symmetric Lévy-stable drivers. In this case, contrary to the popular lore about properties of (Langevin-based) Lévy processes c.f. Refs. [17]-[19] and [20], the pertinent random systems are allowed to relax to (thermal) equilibrium states of a standard Boltzmann-Gibbs form.

The underlying jump-type processes, in the stationary (equilibrium) regime, respect the principle of detailed balance by construction [13]. Their distinctive feature, if compared with the standard Langevin modeling of Lévy flights, is that they have a built-in response *not* to external forces *but rather* to external force potentials. These potentials are interpreted to form confining "potential landscapes" that are specific to the environment. Lévy jump-type processes appear to be particularly sensitive to environmental inhomogeneities, [5, 12].

Lévy flights are pure jump (jump-type) processes. Therefore, it seems useful to indicate that various model realizations of standard jump processes (jump size is bounded from below and above) can be thermalized by means of a specific scenario of an energy exchange with the thermostat. It is based on the *principle of detailed balance*. We have discussed this issue in some detail before [13] along with an extension of this conceptual framework to Lévy-stable processes. Not to reproduce easily available arguments of past publications, we shall be very rudimentary in our motivations.

We quantify a probability density evolution, compatible with a jump-type process on R (this limitation may in principle be lifted in favor of R^n), in terms of the master

equation:

$$\partial_t \rho(x) = \int_{\varepsilon_1 \leq |x-y| \leq \varepsilon_2} [w_\phi(x|y)\rho(y) - w_\phi(y|x)\rho(x)] dy, \quad (1)$$

where ε_1 and ε_2 are, respectively, the lower and upper bounds of jump size and

$$w_\phi(x|y) = C_\mu \frac{\exp[(\Phi(y) - \Phi(x))/2]}{|x-y|^{1+\mu}},$$

$$C_\mu = \frac{\Gamma(1+\mu) \sin(\pi\mu/2)}{\pi} \quad (2)$$

is the jump transition rate from y to x . We stress that $w_\phi(x|y)$ is a non-symmetric function of x and y .

An implicit Boltzmann-type weighting involves a square root of a target pdf $\rho_*(x) \sim \exp[-\Phi(x)]$ and accounts for the a priori prescribed "potential landscape" $\Phi(x)$ whose confining features affect the jump-type process. What matters is a relative impact of a confinement strength of $\Phi(x)$ (level of attraction, see Ref. [7]) upon jumps of the size $|x-y|$, both at the point of origin y and that of destination x . In principle, $\Phi(x)$ may be an arbitrary function that secures a $L^1(\mathbb{R})$ normalization of $\exp(-\Phi(x))$. In this case, the resultant pdf ρ_* is a stationary solution of the transport equation (1) with unbounded jump length, e.g. $\varepsilon_1 \rightarrow 0$ and $\varepsilon_2 \rightarrow \infty$.

We note that the presence of lower and upper bounds of the jump size $\varepsilon_{1,2}$, that are necessary for an implementation of numerical algorithms, enforces a truncation of the jump-type process (without any cutoffs) to a standard jump process. The transition rates of the latter, however, are ruled by Lévy measures of symmetric Lévy stable noises with $\mu \in (0, 2)$. A lower bound for the jump size is usually removed while evaluating the corresponding integrals in the sense of their Cauchy principal values. An upper bound is less innocent and its effects need to be controlled by long tailed pdfs which stands for a distinctive feature of Lévy flights, see a discussion of Lévy stable limits of step processes in Ref. [8]. There is also pertinent discussion of a long time behavior of (unconfined, e.g. free) truncated Lévy flights in Ref. [24].

In contrast to procedures based on the Langevin modeling of Lévy flights in external force fields, [2, 18, 19], there is no known path-wise approach underlying the transport equation (1). With no direct access to sample trajectories of the stochastic process in question, a method must be devised to generate random paths directly from jump transition rates (2). The additional requirement here is that we set a priori a "potential landscape" $\Phi(x)$ for a chosen jump-type (symmetric Lévy stable) noise driver.

The outline of the paper is as follows. First we describe our modification of the Gillespie algorithm which entails a numerical generation of random paths for the dynamics determined by Eqs (1) and (2). Next the statistics of random paths is addressed and various accumulated

data are analyzed with a focus on inherent compatibility issues.

We analyze generic (Cauchy, quadratic Cauchy) and non-generic (Gaussian and locally periodic) examples of target pdfs for the jumping dynamics. Random paths are generated in conjunction with representative Lévy stable drivers, like e.g. those indexed by $\mu = 1/2, 1, 3/2$. Their qualitative typicality is emphasized.

Statistical data, acquired from our modification of Gillespie algorithm, have been employed to generate the dynamical patterns of behavior $\rho(x, t) \rightarrow \rho_*(x)$, to demonstrate the compatibility of the transport (master) equation (1), (2) and its underlying path-wise representation. Both coming from the predefined knowledge of the target pdf and non-symmetric (biased) jump transition rates.

II. RANDOM PATHS: MODIFIED GILLESPIE ALGORITHM.

Here we adopt [25] (and properly adjust to handle Lévy flights) basic tenets of so-called Gillespie's algorithm [21, 22]. Originally, this algorithm had been devised to simulate random properties of coupled chemical reactions. The advantage of the algorithm is that it permits to generate random trajectories of the corresponding stochastic process directly from its (jump) transition rates, with no need for any stochastic differential equation and/or its explicit solution. We emphasize that this feature of Gillespie's algorithm is vitally important, since Langevin modeling is not operational in our framework.

We rewrite Eq. (1) in the form ($x-y=z$)

$$\partial_t \rho(x) = \int_{\varepsilon_1 \leq |z| \leq \varepsilon_2} \left[w_\phi(x|z+x)\rho(z+x) - w_\phi(z+x|x)\rho(x) \right] dz. \quad (3)$$

To construct a reliable path generating algorithm consistent with Eq. (3) we first note that chemical reaction channels in the original Gillespie's algorithm may be reinterpreted as jumps from one spatial point to another, like transition channels in the spatial jump process. An obvious provision is that the set of possible chemical reaction channels is finite (and generically low), while we are interested in all admissible jumps from a chosen point of origin x_0 to any of $[x_0 - \varepsilon_2, x_0 - \varepsilon_1] \cup [x_0 + \varepsilon_1, x_0 + \varepsilon_2]$. It is clear that such jumps form an infinite continuous set. With a genuine computer simulation in mind, we must respect standard numerical assistance limitations. Surely we cannot admit all conceivable jump sizes. As well, the number of destination points, even if potentially enormous, must remain finite for any fixed point of origin.

Our modified version of the Gillespie's algorithm, appropriate for handling of spatial jumps is as follows [26]:

- (i) Set time $t = 0$ and the point of origin $x = x_0$.
- (ii) Create the set of all admissible jumps from x_0 to $x_0 + z$ that is compatible with the transition rate $w_\phi(z + x_0|x_0)$.
- (iii) Evaluate

$$\begin{aligned} W_1(x_0) &= \int_{-\varepsilon_2}^{-\varepsilon_1} w_\phi(z + x_0|x_0) dz, \\ W_2(x_0) &= \int_{\varepsilon_1}^{\varepsilon_2} w_\phi(z + x_0|x_0) dz \end{aligned} \quad (4)$$

and $W(x_0) = W_1(x_0) + W_2(x_0)$.

- (iv) Using a random number generator draw $p \in [0, 1]$ from a uniform distribution.

- (v) Using above p and identities

$$\begin{cases} \int_{-\varepsilon_2}^b w_\phi(z + x_0|x_0) dz = pW(x_0), & p < W_1(x_0)/W(x_0); \\ W_1(x_0) + \int_{\varepsilon_1}^b w_\phi(z + x_0|x_0) dz = pW(x_0), & p \geq W_1(x_0)/W(x_0), \end{cases} \quad (5)$$

find b corresponding to the "transition channel" $x_0 \rightarrow b$.

- (vi) Draw a new number $q \in (0, 1)$ from a uniform distribution.
- (vii) Reset time label $t = t + \Delta t$ where $\Delta t = -\ln q/W(x_0)$.
- (viii) Reset x_0 to a new value $x_0 + b$.
- (ix) Return to step (ii) and repeat the procedure anew.

Comment 1: The original Gillespie algorithm employs a discrete label ν (with a finite range) enumerating possible chemical reactions channels. To identify a channel, one must look for estimates of a double inequality (see Eq. (21b) of Ref. [22])

$$\sum_{\nu=1}^{\mu-1} a_\nu < r_2 a_0 \leq \sum_{\nu=1}^{\mu} a_\nu, \quad a_0 = \sum_{\nu=1}^M a_\nu, \quad (6)$$

where r_2 is a random number, M indicates a total number of chemical reaction channels and $a_\nu dt$ stands for a probability that the ν -th reaction would actually take place in the interval $(t, t + dt)$. To adjust this recipe to our settings, we need to enumerate the infinite number of (infinitely close) channels. This corresponds to passing from summation to integration in Eq. (6). As it has been pointed out above, such situation corresponds to possible transitions from x_0 into an interval $[x_0 - \varepsilon_2, x_0 - \varepsilon_1] \cup [x_0 + \varepsilon_1, x_0 + \varepsilon_2]$. As the Lebesgue measure of a point equals zero, we can replace inequalities by identities in (6), see step (v) of the above algorithm. Formally, we can say that although the number of jumps destinations is finite, their number is so large

that it is consistent to approximate it by a dense subset of intervals $[x_0 - \varepsilon_2, x_0 - \varepsilon_1] \cup [x_0 + \varepsilon_1, x_0 + \varepsilon_2]$. This justifies a replacement of finite sum by an integral over corresponding interval. The following jump size bounds (integration boundaries) were adopted in the numerical procedure: $\varepsilon_1 = 0.001$ and $\varepsilon_2 = 1$.

III. STATISTICS OF RANDOM PATHS: PDF TIME EVOLUTION AND COMPATIBILITY ISSUES.

Our main task in the present section is to select, to some extent generic, transition rates for jump-type processes that will prove to be amenable to the outlined random path generation procedure. Once suitable path ensemble data are collected, we shall verify whether statistical (ensemble) features of generated random trajectories are compatible with the master equation (1). That includes a control of an asymptotic behavior $\rho(x, t) \rightarrow \rho_*(x)$ when $t \rightarrow \infty$.

A. Harmonic confinement (Gaussian target)

Let us consider an asymptotic invariant (target) pdf in the Gaussian form:

$$\rho_*(x) = \frac{1}{\sqrt{\pi}} e^{-x^2}. \quad (7)$$

The corresponding μ -family of transition rates reads

$$w_\phi(z + x|x) = C_\mu \frac{e^{-z^2/2+xz}}{|z|^{1+\mu}}. \quad (8)$$

According to the step (iii) of the simulation algorithm, we must evaluate integrals with transition rates (8) in the intervals $[-\varepsilon_2, -\varepsilon_1]$ and $[\varepsilon_1, \varepsilon_2]$. To execute the step (iv) of the algorithm, we employ the Mersenne-Twister random number generator, [23]. We find b by a numerical solution of the transcendental equation (5) in conformity with step (v) of the algorithm. The C-codes for trajectory generating algorithm, [26], were finally employed to get the trajectory statistics data for three specific choices of Lévy drivers, namely $\mu = 0.5, 1, 1.5$.

Comment 2: For small z , transition rates vary rapidly so that adaptive numerical integration algorithms become very time-consuming. To speed up the calculations, we propose a more efficient procedure (than adaptive numerical integration algorithms with huge number of subdivisions for small z), that amounts to separate integrations for "large" and "small" z subintervals. At small z we can expand the corresponding integrand in Taylor series and truncate it at, say, quadratic term. Generally speaking, the number of terms to be left depends on the accuracy which should be retained during the integration. At "large" z the transition rates vary gradually so that standard adaptive numerical integration works fine.

As an example, we consider the $[\varepsilon_1, \varepsilon_2]$ integration with $\mu = 1$. We set $\varepsilon_{12} = 0.05$, so that for $z \in [\varepsilon_1, \varepsilon_{12}]$ we get

$$\int_{\varepsilon_1}^{\varepsilon_{12}} \frac{e^{-z^2/2 - xz}}{z^2} dz \approx \int_{\varepsilon_1}^{\varepsilon_{12}} \frac{1 - xz + \frac{x^2-1}{2} z^2}{z^2} dz = \frac{\varepsilon_{12} - \varepsilon_1}{2\varepsilon_1\varepsilon_{12}} [2 + (x^2 - 1)\varepsilon_1\varepsilon_{12}] - x \ln \left| \frac{\varepsilon_{12}}{\varepsilon_1} \right|. \quad (9)$$

In the interval $z \in [\varepsilon_{12}, \varepsilon_2]$ we evaluate the integral numerically. The proposed hybrid procedure (integrating analytically in the "most dangerous" small z interval and numerically otherwise) permits to speed up the calculation drastically and has actually been used in our simulations.

The results of our numerical simulations are reported in Figs. 1 through 3. We note, that on Fig. 1 the second moment oscillates near its equilibrium value $1/2$. The oscillations are smoothed out with the growth of the number of random trajectories that contribute to the statistics. A numerical convergence to $\langle X^2 \rangle = 1/2$ is consistent with an analytic equilibrium value of the second moment of the chosen $\rho_*(x)$ (7). The rate of this convergence is higher for larger $\mu \in (0, 2)$. Clearly, for small μ the big jumps are frequent which enlarges the inferred time intervals Δt in the Gillespie's algorithm, see the trajectories on left panel of Fig. 3. Thus, the relaxation to equilibrium is slow. It gets faster for larger μ , when big jumps are rare and time intervals Δt are generically very small.

Fig. 2 displays a probability density evolution, inferred from the ensemble statistics of 75000 trajectories. All of them have started from the same point $x = 0$. Although the data fidelity grows with the number of contributing

paths, we have not found significant qualitative differences to justify a presentation of data for 100 000, 200 000, 250 000 and more trajectories. The relaxation time rate dependence on μ is clearly visible as well. It suffices to analyze differences between three curves for $t = 0.2$ and/or $t = 1$. We observe a conspicuous lowering of their maxima with the growth of μ (take care of different scales on the vertical axes on Fig.2 panels). The simulated pdfs at $t = 10$ are practically indistinguishable from an exact analytical asymptotic pdf (7). The convergence of $\rho(x, t)$ towards $\rho_*(x)$ appears to be relatively fast irrespective of the chosen μ -driver.

Although our reasoning is definitely path-wise and all data have been extracted from trajectory ensembles, it is instructive to visualize generic sample paths. That is accomplished in Fig. 3, basically to indicate their (paths) qualitative typicalities. The structural impact of larger against smaller jumps can be visually compared and has been found to conform with standard simulations of Lévy stable sample paths (with no forces or potentials involved), c.f. [27].

B. Logarithmic confinement

1. Quadratic Cauchy target

Let us consider a long-tailed asymptotic pdf which is a special $\alpha = 2$ case of the one-parameter α -family of equilibrium (Boltzmann-type) states, associated with a logarithmic potential $\Phi(x) \equiv \alpha \ln(1 + x^2)$, $\alpha > 1/2$, see [10–13] :

$$\rho_*(x) = \frac{2}{\pi} \frac{1}{(1 + x^2)^2}. \quad (10)$$

The transition rate (2) $w_\phi(z + x|x)$ for any $\mu \in (0, 2)$ takes the form

$$w_\phi(z + x|x) = \frac{C_\mu}{|z|^{1+\mu}} \frac{1 + x^2}{1 + (z + x)^2}. \quad (11)$$

Similar to the previous Gaussian case, the simulations can be speed up by analytical evaluation of some integrals. Such acceleration of numerical routines permits to handle (in the same timescale) trajectories for much longer running times ($t \sim 400$) than in the previous harmonic case ($t \sim 10$). Each μ -driver case ($\mu = 0.5, 1, 1.5$) will be addressed separately.

Case of $\mu = 1/2$. For $z > 0$ we need to evaluate

$$f_{1/2}(x, z) = \int \frac{1}{z^{3/2}} \frac{1 + x^2}{1 + (z + x)^2} dz. \quad (12)$$

As

$$\frac{1}{z^{3/2}} \frac{1 + x^2}{1 + (z + x)^2} = \frac{1}{z^{3/2}} - \frac{2x + z}{\sqrt{z} [1 + (z + x)^2]}, \quad (13)$$

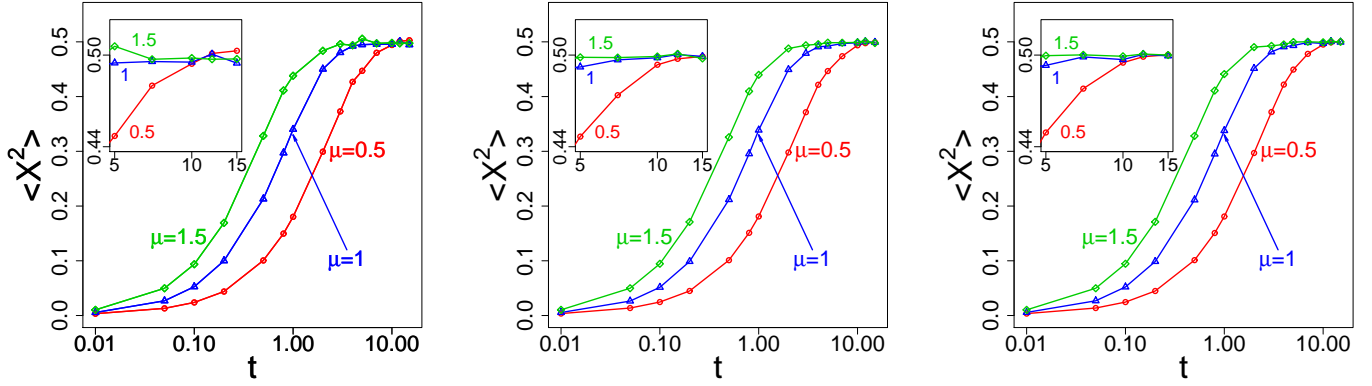


FIG. 1: Gaussian target: Time evolution of the pdf $\rho(x, t)$ second moment for 25 000 (left panel), 50 000 (middle panel) and 75 000 (right panel) trajectories. Insets visualize the oscillations smoothing in the asymptotic regime for $10 \leq t \leq 15$; figures near curves correspond to μ values.

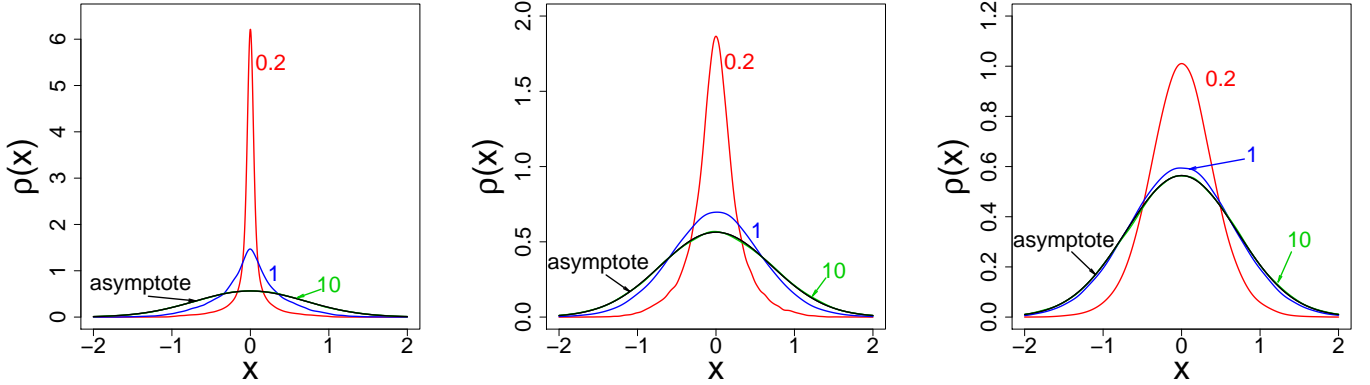


FIG. 2: Gaussian target: Time evolution of $\rho(x, t)$ inferred from 75 000 trajectories: $\mu = 0.5$ (left panel), $\mu = 1$ (middle panel) and $\mu = 1.5$ (right panel). All trajectories originate from $x = 0$, i.e. refer to the $\delta(x)$ -type initial probability distribution.

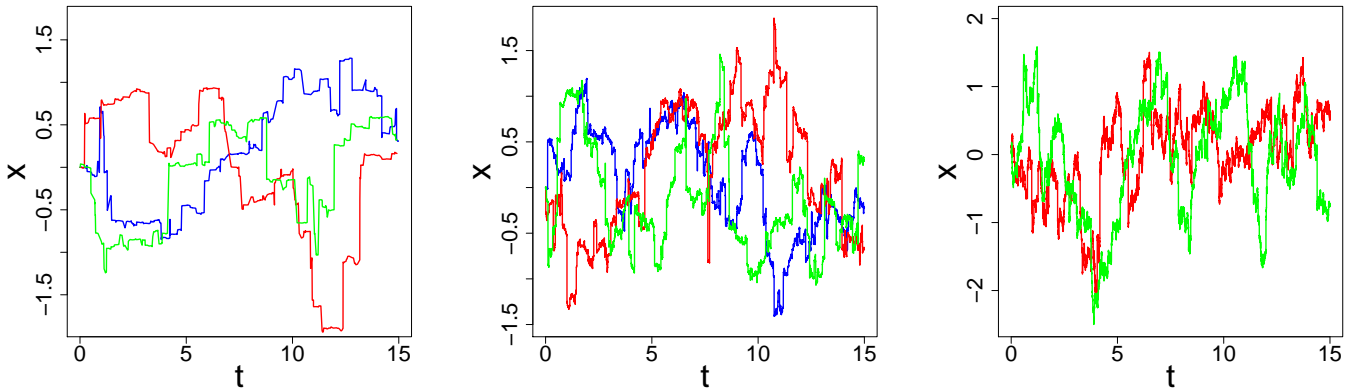


FIG. 3: Gaussian target. Qualitative typicalities of sample paths for $\mu = 0.5$ (left panel), $\mu = 1$ (middle panel) and $\mu = 1.5$ (right panel). All trajectories originate from $x = 0$. Right panel comprises two trajectories instead of three (for better visibility).

$f_{1/2}(x, z)$ can be written as

$$f_{1/2}(x, z) = -2z^{-1/2} - \int \frac{2x+z}{\sqrt{z}(1+(x+z)^2)} dz. \quad (14)$$

For small z the dominant contribution comes from the first term so that the second term can efficiently be evaluated numerically. We note here that although the in-

$$f_1(x, z) = \int \frac{1+x^2}{1+(z+x)^2} \cdot \frac{dz}{z^2} = \frac{x}{1+x^2} \ln(1+(z+x)^2) + \frac{x^2-1}{x^2+1} \arctan(z+x) - \frac{2x}{1+x^2} \ln|z| - \frac{1}{z}. \quad (15)$$

We pay attention to the fact that the integrand is rational, hence the integral can be evaluated analytically in a simple form. This permits to use the analytical answer (15) in our simulations without the need to divide the integration range into "small" and "large" z domains.

Case of $\mu = 3/2$. In this case, we have for $z > 0$

$$f_{3/2}(x, z) = \int \frac{1}{z^{5/2}} \frac{1+x^2}{1+(z+x)^2} dz. \quad (16)$$

Since

$$\frac{1}{z^{5/2}} \frac{1+x^2}{1+(z+x)^2} = \frac{1}{z^{3/2}} \left(\frac{1}{z} - \frac{2x+z}{1+(z+x)^2} \right), \quad (17)$$

there holds

$$f_{3/2}(x, z) = -\frac{2}{3z^{3/2}} + \frac{4x}{(1+x^2)z^{1/2}} + \int \frac{2xz+3x^2-1}{(1+x^2)(1+(z+x)^2)z^{1/2}} dz. \quad (18)$$

Again, the third term in (18) can efficiently be evaluated numerically. For $z < 0$ we encounter $-f_{3/2}(-x, -z)$.

Simulation results are displayed in Figs. 4 and 5. If we compare Fig. 4 with Fig. 1 we see the existence of small oscillations in the asymptotic regime about the value $1/2$. Those from Fig.1 were relatively small and were quickly smoothed out with the growth of the number of trajectories used to extract statistical data. In Fig. 4 the oscillations are more noticeable and persist even for 200000 trajectories and more. This is related to much

tegration in the second term of (14) can be performed analytically, the result appears to be quite cumbersome. Therefore, for our purposes it is more profitable to integrate this term numerically. For $z < 0$ the corresponding integral can be expressed as $-C_\mu f_{1/2}(-x, -z)$.

Case of $\mu = 1$. Here, we need to evaluate the integral

slower decay of transition rates (11) (determined by slow-decaying asymptotic pdf (10)) as compared to those for Gaussian case (8).

The second moment of the present $\rho_*(x)$, (10), equals 1 and the convergence towards this value is clearly seen in Fig. 3. This convergence is much slower than in the Gaussian (harmonic confinement) case which is not a surprise: (8) and (11) indicate that the present rate of convergence should be logarithmically slower. Fig. 5, quite alike Fig. 2, convincingly demonstrates a convergence of $\rho(x, t)$ to the asymptotic $\rho_*(x)$. For definitely large times around $t = 400$, $\rho(x, t)$ and $\rho_*(x)$ become practically indistinguishable. Similarly to the Gaussian case, the rate of convergence becomes larger with the growth of $\mu \in (0, 2)$.

2. Cauchy target

Now we consider an asymptotic pdf of the form :

$$\rho_*(x) = \frac{1}{\pi} \frac{1}{1+x^2}. \quad (19)$$

In this case, the transition rate from x to $x+z$ reads

$$w_\phi(z+x|x) = \frac{C_\mu}{|z|^{1+\mu}} \sqrt{\frac{1+x^2}{1+(z+x)^2}}. \quad (20)$$

We consider Cauchy driver corresponding to $\mu = 1$. The transition rate integral can be evaluated analytically. For $z > 0$ we have

$$f(x, z) = \int \sqrt{\frac{1+x^2}{1+(z+x)^2}} \cdot \frac{dz}{z^2} = \frac{-\sqrt{1+x^2}\sqrt{1+(z+x)^2} + xz \ln\left(\frac{(1+x^2+zx+\sqrt{1+x^2}\sqrt{1+(z+x)^2})/z}{(1+x^2)}\right)}{(1+x^2)z}. \quad (21)$$

For $z < 0$ the outcome is $-f(-x, -z)$.

In Fig. 6, we report the time evolution of the statistically inferred $\rho(x, t)$, its half-width (as second moment

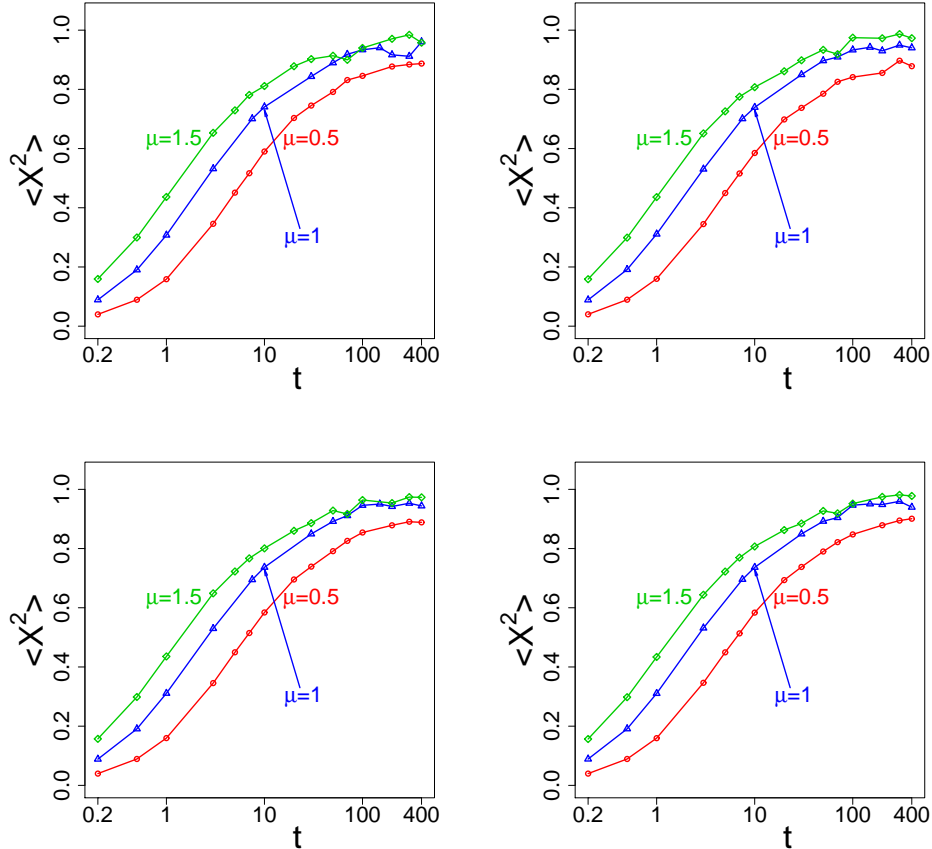


FIG. 4: Quadratic Cauchy target: Time evolution of the pdf $\rho(x, t)$ second moment for 50 000 (upper left panel), 100 000 (upper right panel), 150 000 (lower left panel) and 200 000 (lower right panel) trajectories.

does not exist for asymptotic pdf (19)) and simulated cumulative probability distributions (CPD) for different time instants. An approach to the asymptotic pdf (19) is clearly seen, together with a convergence of a half-width to its asymptotic value 1. The same convergence pattern is observed for CPD which approaches the asymptotic function $F(x) = \frac{1}{2} + \frac{\arctan x}{\pi}$.

Comment 3: Displayed empirical (numerically retrieved) curves in Fig. 6 are hampered by certain errors. The figures have been read from a histogram of randomly sampled data. Its partitioning into subintervals is a source of inaccuracies. In case of a small number of intervals, the read-out error would be large, with a size of about half-interval length. A finer partitioning (large number of small subintervals) would still produce an error which is close to the half-maximum of the curve. The error bound would be smaller or equal to the half-length of subintervals corresponding to roughly the same histogram values. One more inaccuracy source in the finer partition case comes from the maximum read-out imprecision. Namely, we can have a conspicuous peak, whose close vicinity displays much (half or less) smaller values. Therefore the partitioning finesse must be slightly opti-

mized.

C. Locally periodic confinement

To set firm grounds for future research it is instructive to study our model for more complicated forms of confining potentials. In view of their physical relevance, it is appealing to address an issue of confining (trapping) environments with a periodic spatial structure. Here, we encounter a major difficulty with a $L^1(R)$ integrability of the Boltzmann-type weighting function $\exp(-\Phi)$. Periodicity and integrability can here be reconciled either on compact sets or by means of locally periodic potentials that take a definite confining form (harmonic or polynomial) for larger values of $x \in R$. Let us consider the following asymptotic pdf

$$\rho_*(x) = \begin{cases} \frac{1}{C} e^{-\sin^2(2\pi x)}, & |x| \leq 2; \\ \frac{1}{C} e^{-(x^2-4)}, & |x| > 2, \end{cases} \quad (22)$$

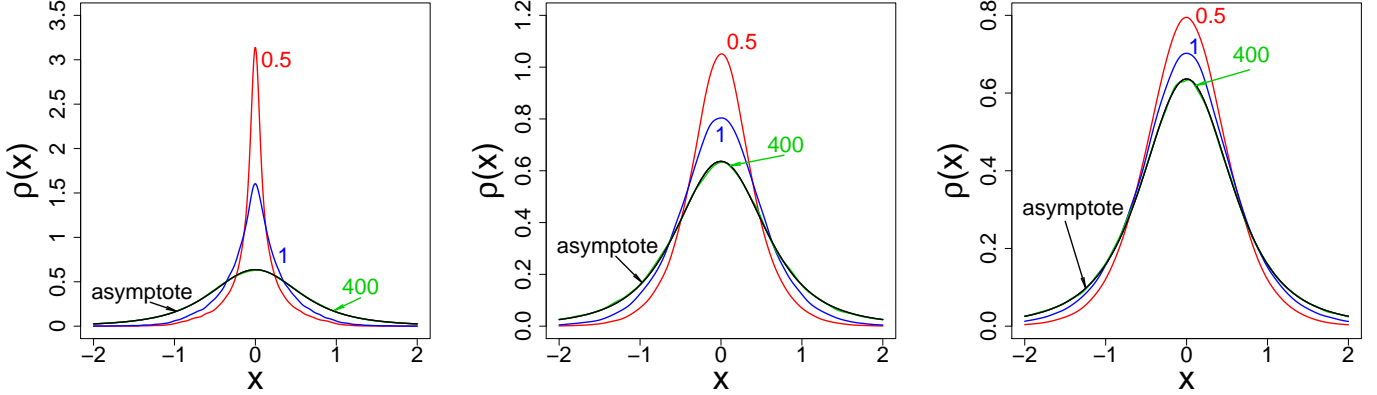


FIG. 5: Quadratic Cauchy target: Time evolution of $\rho(x, t)$ inferred from 200000 trajectories for $\mu = 0.5$ (left panel), $\mu = 1$ (middle panel) and $\mu = 1.5$ (right panel). All trajectories are started from $x = 0$. Note scale differences on vertical axes.

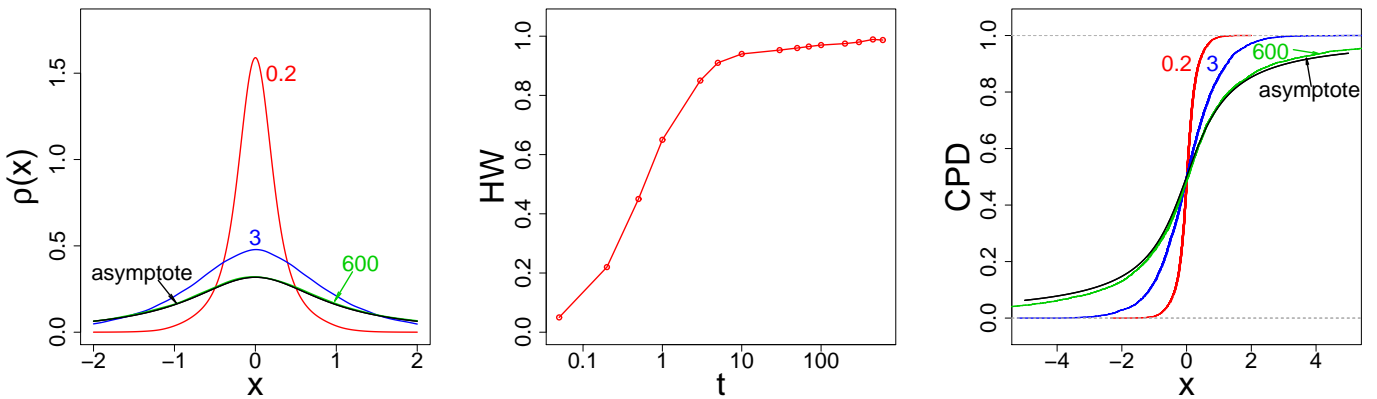


FIG. 6: Cauchy target: Time evolution of pdf $\rho(x, t)$ (left panel), half-width (HW) of $\rho(x, t)$ (middle panel). Right panel reports the cumulative probability distributions (CPD) for different time instants. Here $\mu = 1$ and all data are inferred from 200000 trajectories, starting from $x = 0$.

where $C = 3.032818$ is a normalization constant. The transition rate from x to $x + z$ reads

$$w_\phi(z + x|x) = \frac{C_\mu}{|z|^{1+\mu}} \exp[(\phi(x) - \phi(x+z))/2], \quad (23)$$

where the potential ϕ has the form

$$\phi(x) = \begin{cases} \sin^2(2\pi x), & |x| \leq 2; \\ (x^2 - 4), & |x| > 2. \end{cases} \quad (24)$$

We consider $\mu = 1$. To optimize the simulation, here we use the same trick of isolating of "most danger-

ous" small z terms in the integrals involved in the Gillespie algorithm. For small z we expand the term $\exp[(\sin^2(2\pi x) - \sin^2(2\pi(x+z)))/2]$ in Taylor series. We choose $\varepsilon_{12} = 0.05$. In the vicinity of $|x| = 2$ due attention must be paid to the proper power series truncation, to correctly choose the intervals where integration should be performed numerically. For example at $x \in (1.95, 2)$ we have

$$\begin{aligned}
\frac{1}{C_1} \int_{\varepsilon_1}^{\varepsilon_{12}} w_\phi(z+x|x) dz &= \int_{\varepsilon_1}^{2-x} \exp \left[\frac{\sin^2(2\pi x) - \sin^2(2\pi(x+z))}{2} \right] \frac{dz}{z^2} + \int_{2-x}^{\varepsilon_{12}} \exp \left[\frac{\sin^2(2\pi x) - (x+z)^2 + 4}{2} \right] \frac{dz}{z^2} \\
&= \int_{\varepsilon_1}^{2-x} \exp \left[\frac{\sin^2(2\pi x) - \sin^2(2\pi(x+z))}{2} \right] \frac{dz}{z^2} + \exp \left[\frac{\sin^2(2\pi x) - x^2 + 4}{2} \right] \int_{2-x}^{\varepsilon_{12}} \exp \left[\frac{x^2 - (x+z)^2}{2} \right] \frac{dz}{z^2}. \quad (25)
\end{aligned}$$

The numerators of integrand fractions have been expanded into Taylor series and (safely) truncated at the quadratic terms.

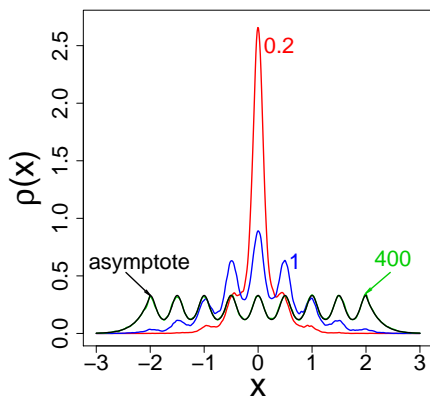


FIG. 7: Time evolution of $\rho(x, t)$ inferred from 200000 trajectories at $\mu = 1$. The data for 100000 and 300000 trajectories (not displayed) do not show qualitative differences.

Time evolution of the inferred pdf $\rho(x, t)$ is reported in Fig. 7. All sample trajectories were started from $x = 0$ which corresponds to the $\delta(x)$ -type initial distribution. The probability density spreads out with time in conformity with the trapping (confining) properties of the locally periodic enclosure (environment or "potential landscape"). For large running times $t=400$ the trajectory statistics produces data that are indistinguishable from those for the asymptotic pdf. We have checked that beginning from about 100 000 trajectories, further accumulation of the trajectories number like e.g. 200 000 (displayed) and 300 000 (not displayed) for the data statistics is inessential. In such cases the curves are almost the same, we merely improve a fidelity of the statistics.

IV. CONCLUSIONS

If a random process does not admit the description in terms of a stochastic differential equation (e.g. Langevin modeling), its direct numerical simulation becomes impossible by means of existing popular algorithms. In the

present paper, for the first time in the literature, we propose a working method to generate stochastic trajectories (sample paths) of a random jump-type process without resorting to any explicit (or numerical) solution of a stochastic differential equation. To this end we have modified the Gillespie algorithm [21, 22], normally devised for sample paths generation if the transition rates refer to a finite number of states of a system.

The essence of our modification is that we take into account the continuum of possible transition rates, thereby changing the finite sums in the original Gillespie algorithm into integrals. The corresponding procedures for stochastic trajectories generation has been changed accordingly. In other words, here we "extract" the background sample paths of a jump process, whose pdf obeys the transport equation (generalized Fokker-Planck dynamics) (1), (2). We emphasize once more here, that we have focused on those background jump-type processes that cannot be modeled by any stochastic differential equation of the Langevin type.

Although heavy-tailed Lévy stable drivers were involved in the present considerations, we have clearly confirmed that an enormous variety of stationary target distributions is dynamically accessible in each particular $\mu \in (0, 2)$ case. That comprises not only a standard Gaussian pdf, casually discussed in relation to the Brownian motion (e.g. the Wiener process). Among heavy-tailed distributions, we have paid attention to the Cauchy pdf which can stand for an asymptotic target for any $\mu \neq 1$ driver, provided a steering environment is properly devised. In turn, the Cauchy driver in a proper environment may lead to an asymptotic pdf with a finite (in fact arbitrarily large) number of moments, the Gaussian case being included ([13]).

An example of the locally periodic environment has been considered as a toy model for more realistic physical systems. Our major hunch are strongly inhomogeneous "potential landscapes", [12], being sufficiently smooth to avoid a direct reference to random potentials, [6]. Even if various mean field data are available in such (experimentally realizable) systems, it is of interest to have some knowledge about the microscopic dynamics (random paths) for the system under consideration. The detailed analysis of sample path data (ergodicity, mixing or lack of those properties) deserve a separate analysis.

We mention possible generalizations of our method to the Brownian motor concept (see, e.g., Ref. [28] for re-

cent review) to include a non-Gaussian jumping component. In those systems it is the properly tailored periodic "potential landscape" which enforces a conversion of a homogenous stochastic process (Brownian motion for reference) into the directed motion of particles at nanometer scales. That is closely related to the problem of so-called sorting in periodic potentials [29]. Other problem to be addressed concerns ultracold atoms in optical lattices subject to random potentials [30], which might promising not only from a purely scientific point of view, but also with prospects for many technological applications. We note that the theoretical description of the above mentioned topics relies essentially on the Langevin-like equation input.

Our approach offers an immediate generalization for generalizations, where systems with non-Langevin response to external potentials may come into consideration, along with more traditional ones. What we actually

need to implement our version of Gillespie's algorithm is the knowledge of jump transition rates of those random systems only.

A preliminary work (in progress) shows that an extension of our algorithm to higher dimensions is operational. In particular, the planar case is worth exploration, possibly with more complex "potential landscapes". While departing from final comments of Ref. [12] we expect that the presented methodology can be effectively adopted to construct optimal random search routines, see in this connection [31].

Acknowledgement: P. G. would like to thank Igor M. Sokolov for indicating a possible relevance of the Gillespie's algorithm out of its original chemical kinetics context. All numerical simulations were completed by means of the facilities of the Platon - Science Services Platform of the Polish Pionier Network.

-
- [1] H. Risken, *The Fokker-Plack Equation*, (Springer-Verlag, Berlin, 1989)
- [2] S. Jespersen, R. Metzler and H. C. Fogedby, *Phys. Rev. E* **59**, 2736, (1999)
- [3] R. Metzler, J. Klafter *J. Phys. A:Math. Gen.* **37**, R161, (2004)
- [4] L. Chen and M. W. Deem, *Phys. Rev. E* **65**, 011109, (2001)
- [5] D. Brockmann and I. M. Sokolov, *Chemical Physics*, **284**, 409, (2002)
- [6] D. Brockmann and T. Geisel, *Phys. Rev. Lett.* **90**, 170601, (2003)
- [7] V. V. Belik and D. Brockmann, *New. J. Phys.* **9**, 54, (2007)
- [8] P. Garbaczewski and R. Olkiewicz, *J. Math. Phys.* **40**, 1057, (1999)
- [9] P. Garbaczewski and R. Olkiewicz, *J. Math. Phys.* **41**, 6843, (2000)
- [10] P. Garbaczewski and V. A. Stephanovich, *Phys. Rev. E* **80**, 031113, (2009)
- [11] P. Garbaczewski and V. Stephanovich, *Open Systems & Information Dynamics*, **17**, 287, (2010)
- [12] P. Garbaczewski and V. A. Stephanovich, *Physica A* **389**, 4410, (2010)
- [13] P. Garbaczewski and V. Stephanovich, *Phys. Rev. E* **84**, 011142 (2011)
- [14] J. Lőrinczi, F. Hiroshima and V. Betz, *Feynman-Kac-Type Theorems and Gibbs Measures on Path Space*, (Studies in Mathematics **34**, Walter de Gruyter, Berlin, 2011)
- [15] R. Vilela Mendes, *J. Math. Phys.* **27**,178, (1986)
- [16] S. Eleutério and R. Vilela Mendes, *Phys. Rev. B* **50**, 5035, (1993).
- [17] I. Eliazar and J. Klafter, *J. Stat. Phys.* **111**, 739, (2003)
- [18] V. V. Janovsky et al., *Physica A* **282**, 13, (2000)
- [19] A. Dubkov and B. Spagnolo, *Fluct. Noise Lett.* **5**, L267, (2005)
- [20] H. Touchette and E. G. D. Cohen, *Phys. Rev. E* **76**, 020101, (2007)
- [21] T. D. Gillespie, *J. Phys. Chemistry*, **81** (25): 2340, (1977)
- [22] T. D. Gillespie, *J. Comput. Physics*, **22** (4): 403, (1976)
- [23] M. Matsumoto and T. Nishimura, *ACM Trans. Model. Comput. Simul.* **8**, 3 (1998)
- [24] R. N. Mantegna and H. E. Stanley, *Phys. Rev. Lett.* **73**, 2946, (1994)
- [25] I. M. Sokolov, private communication
- [26] C-code is available upon request
- [27] A. Janicki and A. Weron, *Simulation and chaotic behavior of α -stable stochastic processes*, (M. Dekker, New York, 1994)
- [28] P. Hänggi, F. Marchesoni *Rev. Mod. Phys.* **81**, 387, (2009)
- [29] S. I. Denisov, T. V. Lyutyy *et al* *Phys. Rev. E* **79**, 051102, (2009)
- [30] H. Gimperlein, S. Wessel, J. Schmiedmayer, and L. Santos *Phys. Rev. Lett.* **95**, 170401, (2005)
- [31] J. Snider, *Phys. Rev. E* **83**, 011105, (2011)